NAGW-49

GEOPHYSICAL RESEARCH LETTERS, VOL. 24, NO. 17, PAGES 2183-2186, SEPTEMBER 1, 1997

NASA/CR-97- 207139

Topography of the lunar south polar region: Implications for the size and location of permanently shaded areas

Maria T. Zuber[1]

Department of Earth, Atmospheric and Planetary Sciences, Massachusetts Institute of Technology, Cambridge, Massachusetts

David E. Smith

Laboratory for Terrestrial Physics, NASA/Goddard Space Flight Center, Greenbelt, Maryland

Abstract. We analyze Clementine altimetry to constrain the size and location of proposed permanently shadowed regions in the vicinity of the lunar south pole. Long and short wavelength topography in the vicinity of the pole, in combination with measurements of depths of well-preserved craters and basins and the lunar topographic power spectrum, have direct bearing on the nature of elevations in the south polar region. A criterion based on geometric considerations and altimetry demonstrates that the existence of permanent shadowing is not very sensitive to the elevation of the south pole. In addition, permanent shadowing cannot be a consequence of large structures such as the South Pole-Aitken Basin and/or a 300-km degraded polar basin. Perennially dark regions, if they exist, are most likely associated with craters or other axisymmetric features with diameters of at most 80 km centered at the pole. For structures displaced 2° from the pole the maximum allowable diameter decreases to ~30 km.

Introduction

The recent possible detection of water ice at the lunar south pole from the Clementine bistatic radar experiment [*Nozette et al.*, 1996] has potentially major implications for future lunar exploration initiatives. The basis for the potential finding is the recognition of backscatter and polarization enhancement of radar echoes transmitted by the spacecraft that interacted with a region of the lunar surface near the pole, outlined in Fig. 1. The unusual radar signature has been interpreted as being due to coherent backscatter of a high volume scattering substance, most likely water ice [*Nozette et al.*, 1996], though lunar surface roughness near the radar wavelength has been offered as an alternative explanation on the basis of analysis of higher spatial resolution Earth-based observations [*Stacy et al.*, 1997]. The retention of near-surface ice, presumably deposited by cometary or asteroidal impacts, would require areas of the lunar surface to have been shadowed from sunlight over geological timescales [*Watson et al.*, 1961; *Arnold*, 1979; *Ingersoll et al.*, 1992].

Continuous shadowing in the lunar south polar region has been identified on the basis of the Clementine south pole image mosaic [*Shoemaker et al.*, 1994; *Spudis et al.*, 1995], which was assembled from two months of orbital imaging. However, dark regions in the mosaic do not necessarily imply permanent shadowing [*Shoemaker et al.*, 1994]. The Clementine observations were obtained during southern hemisphere winter, when the tilt of the Moon's rotation axis was ~1.5° from pole of the ecliptic in the direction away from the sun. An increase of the sun's elevation above the south polar horizon of over 3° will occur during southern summer at some time during the year, and it is probable that at least some of the darker areas seen in the Clementine mosaic will then be illuminated.

Surface topography, defined as elevation with respect to the geoid, is another essential observation required to distinguish the location and physiographic context of permanently shadowed regions. Unfortunately a definitive analysis of topographic constraints is not possible because there are currently no direct measurements of lunar topography at either pole. However, there are well-constrained indirect topographic observations that provide insight into the distribution and character of south polar elevations. These include: long wavelength lunar topography, near-polar short wavelength topography, measured depths of craters and basins distributed over the lunar surface, and the global topographic power spectrum. Because of the unique contribution of

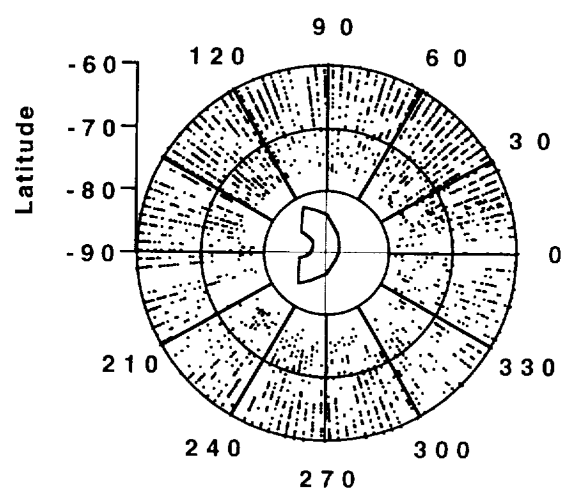

Figure 1. Distribution of surface elevations from Clementine altimetry between latitude -60° and the south pole. The semi-circular area near the pole is the region of enhanced radar backscatter recognized by *Nozette et al.* [1996]. Proposed regions of permanent shadowing within this area have been interpreted as containing ice and/or other frozen volatiles [*Nozette, et al.*, 1996]. In the figure the direction of Earth is to the right.

[1]Also at : Laboratory for Terrestrial Physics, NASA/Goddard Space Flight Center, Greenbelt, Maryland.

Paper number 97GL02111.
0094-8534/97/97GL-02111$05.00

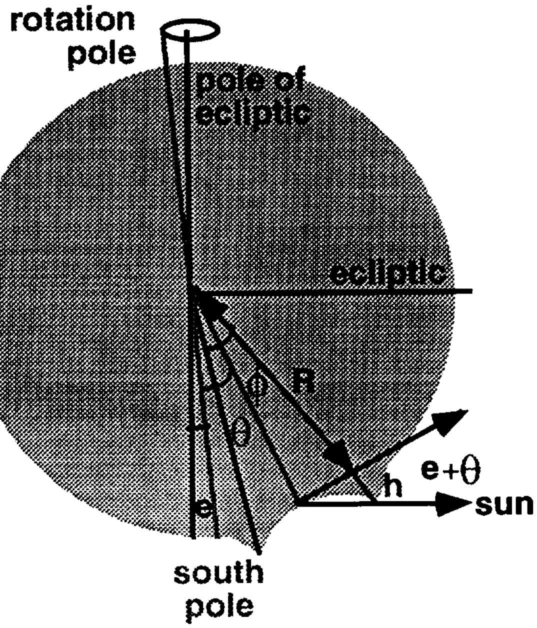

Figure 2. Schematic of geometric criterion for permanent shadowing.

topography to assessing objectively whether ice exists on the Moon, we have analyzed the relevant aspects of the Clementine altimetry and present an evaluation of the extent to which the location and size of possible permanently shadowed regions can be clarified and quantified.

Necessary Topographic Conditions for Permanent Shadowing

Regions near the south pole that are in permanent darkness must be surrounded on all sides by topography that blocks sunlight at all times. This suggests quasi-axisymmetric structures that cause shadowing of an area from all sides and from all solar directions. However, as illustrated by the oblong-shaped anomalously bright radar feature at Mercury's north pole that is thought to contain water ice [*Harmon and Slade*, 1992], shadowing configurations that arise at least in part from random topography cannot be excluded. If the structure is not symmetric the surrounding topography will need, in general, to be higher. Of possible axisymmetric structures, the geometry and abundant distribution of craters and basins makes them by far the most likely candidate structures. Further, the tops of shadowing structures must in all probability be sunlit, at least part of the time. If shadowing comes instead from a larger, exterior structure, then a higher topographic elevation for shadowing will be required.

A further constraint comes from the Moon's axial tilt. The angle between the Moon's rotation axis and the pole of the ecliptic of 1.54° plus the physical libration in latitude of 0.04° [*Dickey et al.*, 1994] enables the sun, as seen by an observer at the pole, to reach an elevation of 1.58° above the horizon from all directions during southern summer. For the pole to be in darkness the elevation angle *(e)* of the topographic horizon at the pole must be at least 1.58° plus the apparent radius of the sun (0.27°) in all directions. So for an area at the pole to be in permanent darkness over the timescale of the 18.6-year lunar precession period e must exceed 1.85°. As shown schematically in Fig. 2, if the shadowing structure is not centered on the pole an additional term for the co-latitude, θ, must be included. The horizon elevation, h, required for permanent shadowing is

$$h = R\left[\frac{\cos(e+\theta)}{\cos(e+\theta+\phi)} - 1\right] \tag{1}$$

where ϕ is the angular distance of the shadowing structure (*i.e.* crater rim) to a shadowed point, and R is the radius of the lunar geoid.

Data

Our analysis utilizes the best current topographic dataset for the Moon -- 72,548 radius measurements [*Smith et al.*, 1997] obtained from the Clementine LIDAR [*Nozette et al.*, 1994]. These radii, which have an absolute vertical accuracy of ~100 m with respect to the Moon's center of mass [*Zuber et al.*, 1994], were derived from laser ranges to the lunar surface along the spacecraft ground tracks. Fig. 1 shows that the LIDAR collected successful range measurements as far south as latitude -79°, and there are 752 radius measurements south of -70°. At latitude -70° the along-track resolution, in tracks where there is data, is approximately 20 km, while at -75° the along-track resolution decreases to 60 km. The across-track resolution is governed by the spacing of spacecraft orbital tracks and is ~10 km in the relevant latitude range. Fig. 1 also shows the ~25° (3×10^5 km^2) data gap centered approximately on the south pole, with the region of enhanced Clementine radar backscatter shown as a quasi-crescent area at the center. *Nozette et al.* [1996] propose that this area contains a region or regions of permanent shadowing with a surface area of at least 6361 km^2, the approximate cross-sectional equivalent of a 90-km diameter crater.

Topography Analysis

Fig. 3 plots six profiles of surface elevation relative to the mean lunar radius along meridional planes that cross the south pole and the deepest part of the massive South Pole-Aitken Basin. The figure illustrates that South Pole-Aitken dominates broad-scale southern hemisphere topography, even in the vicinity of the pole. *Nozette et al.* [1996] invoked a low polar elevation (-4 to -7 km relative to the mean), due to location of the pole within South Pole-Aitken, to explain the presence of permanent shadowing. From Fig. 3 we see that estimation of the south polar elevation requires interpolation over the polar gap. Based on analysis of all southern hemisphere profiles that contain high latitude data as well as a spherical harmonic expansion of all the Clementine altimetry [*Smith et al.*, 1997], we find that the best-fit elevation is probably shallower, -1±2 km, with the large uncertainty a consequence of the interpolation. In addition, small craters at the pole may make the elevation locally deeper. However, equation (1) indicates that the polar elevation is only one of several factors that have bearing on the existence of permanent shadowing. Fig. 4 plots equation (1) and shows how the height of encircling topography also depends on the angles ϕ and θ. The plot assumes a radius of the lunar geoid of 1738 km, but even kilometer-scale uncertainties due to the data gap at the south pole result in small (meter to tens of meter) variations in the required topographic height. Equation (1) dictates that the existence of permanent shading is less sensitive to the range of possible polar elevations *(R)* than to the size of a shadowing structure and its distance from the pole

Consider the case of the South Pole-Aitken Basin. Fig. 4 shows that the amplitude of topography required for permanent shadowing for a structure of its size, centered on the pole, would be more than 30 km -- over a factor of two greater than the full dynamic range of lunar topography and four times the depth of the basin. Fig. 4 also plots the depths of the best preserved complex craters and basins on the Moon. These data show that structures with diameters less than 80 km (~2.6°)

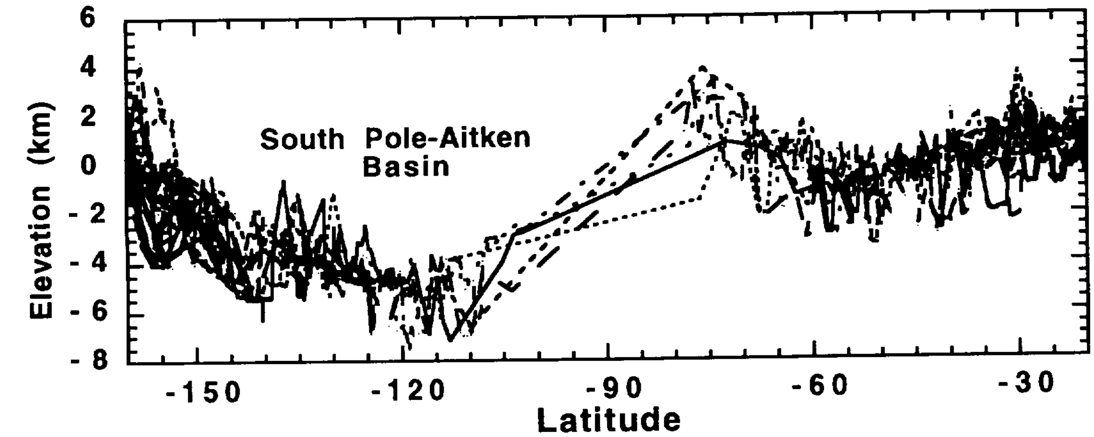

Figure 3. Profiles of surface elevation derived from Clementine altimetry along six meridional planes through the lunar south pole. The profiles pass through the South Pole-Aitken Basin (longitudes 200°-250°) at its deepest part, showing the maximum depth of the basin. Individual data points are plotted. Note that the profiles have been interpolated through the polar gap in altimetric coverage. All other Clementine profiles indicate a larger interpolated radius of the pole.

would meet the topographic amplitude criterion for permanent shadowing if they are centered on the pole. *Shoemaker et al.* [1994] identified an ancient, largely obliterated ~300-km diameter basin that nearly directly overlies the south pole.

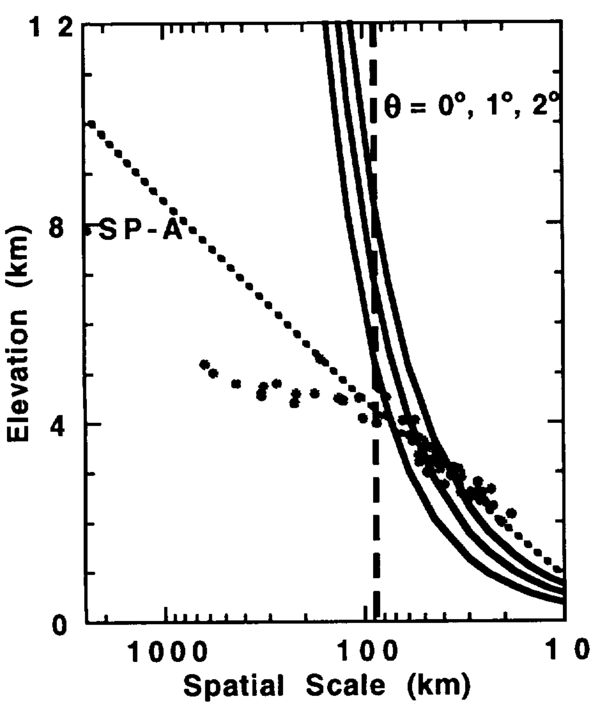

Figure 4. Plot of elevation vs. log(spatial scale). Solid lines correspond to the horizon elevation required for permanent shadowing (equation 1). Solutions are shown for co-latitudes θ of 0° (the pole), 1° and 2°. The grey dots show depths of well-preserved lunar complex craters [*Pike*, 1974] and basins [*Williams and Zuber*, 1997], including the South Pole-Aitken Basin (SP-A). The dotted line represents the integral of the lunar topographic power spectrum (equation 2) from degree 1000 (spatial scale of 5 km) through degree 2 (2730 km). The vertical line corresponds to the crater diameter of the equivalent cross-sectional area of the lower size limit of the region of proposed permanent shadow [*Nozette, et al.*, 1996].

However, the basin size and corresponding predicted depth, even if it were not visibly degraded, dictate that this structure cannot produce permanent shadowing.

The lunar topographic power spectrum is well-described by the empirical relation

$$rms(h) = \frac{2000}{N^{1.05}} \qquad (2)$$

where N is the spherical harmonic degree and h has units of meters. The power law, which has an RMS fit to the observed power of 11%, was derived from a spherical harmonic model of the topography out to degree 70 (spatial scales <78 km) [*Smith et al.*, 1997]. The spectrum shows that, as for the other terrestrial planets [*Turcotte*, 1987], lunar topography displays a fractal distribution. The dotted line in Fig. 4 shows the predicted topography signal obtained by extrapolating and integrating equation (2) from degrees 1000 through 2. The integrated topographic power suggests that the maximum diameter of a structure centered on the pole that can produce permanent shadowing is about 68 km. If a structure is centered 2° off the pole, as is the apparent region of constant shadowing in the Clementine south pole mosaic, the maximum allowable diameter decreases to about 33 km.

The dashed line in Fig. 4 corresponds to the spatial scale implied if the minimum size of the region of permanent shadowing identified by *Nozette et al.* [1996] is confined to a single crater. The intersection of the line with the family of curves representing the geometric criterion for shadowing shows that a crater of that size, if centered on the pole, would require surrounding topography of order 5 km. This amplitude is greater than suggested by either the observed crater depth data or the integrated topographic power spectrum. If the structure is centered 2° off the pole over 8 km of topography would be required, at least in some places, for permanent shadowing. Thus, to explain the areal extent of permanent shading provisionally identified by *Nozette et al.* requires that shadowing be distributed in more than one zone, as multiple smaller structures would allow lower topography.

Discussion and Conclusions

The criterion we have adopted is more permissive of permanent shadowing than a more rigorous assessment would allow. Indeed our analysis addresses only the larger geometric effects. First, we have ignored variations in the direction of the lunar spin axis over timescales longer than the lunar precession cycle, although such variations are believed to have occurred [*Newhall et al.*, 1983], and may have been dramatic [*Ward*, 1975]. Second, we do not consider the possibility of solar illumination of an area via secondary reflections off surface topography. Third, we have not considered the thermal conditions required for retention of a given volatile species within an area of permanent shadowing, although other studies have demonstrated the plausibility of entrapping and retaining over geologic timescales cometary ice in perennially dark lunar cold traps [*Ingersoll et al.*, 1992; *Paige et al.*, 1992; *Salvail and Fanale*, 1994]. Such analysis could profitably be revisited taking into account the improved topographic understanding of the region.

In support of our use of indirect observations to understand the nature of near-polar topography, we note the correspondence of the slope of the depth/diameter ratios of complex craters with that of the integrated power spectrum. The near overlap of the relationships, we believe, is not accidental, but rather an indication that in the coincident wavelength range the complex craters dominate the topographic power. It also suggests that the power spectrum is indeed representative of the topographic power of the Moon in this range of spatial scales, which happens to be the length scale range relevant to structures that could cause permanent shadowing.

Even given the simplicity of our analysis it is clear that placement within the confines of large structures such as the South Pole-Aitken Basin and/or the 300-km ancient south polar basin identified by *Shoemaker et al.* [1994] are insufficient conditions for permanent shadowing. Further, the increase in solar elevation of over 3° at southern lunar summer as compared to the time of the Clementine observations taken during southern winter are likely to have a profound effect on the shadowing patterns near the south pole. Consequently, we expect shadowing at the south pole during southern summer to look more like shadowing seen at the north pole during northern summer. The lunar north polar region was observed by Clementine during northern summer and showed more limited shadowing (~530 km^2) than at the south pole over the two months of mapping [*Nozette et al.*, 1996].

Zones of perennial darkness at either lunar pole are constrained in a topographic sense to occur within craters of at most 80-km diameter, and probably significantly less. Without actual topographic data for the lunar south pole region or imaging over a much longer period than mapped by Clementine it is impossible to either verify or reject conclusively the existence of permanent shadowing. But from the data at hand it appears that if permanently dark regions do exist they are likely to be constrained to a very small total area, probably within small fresh craters, very close to the lunar pole. A 15-km diameter crater, nearly centered at the south pole, is an obvious candidate structure (E. Shoemaker, personal communication, 1997). This and other structures that meet the topographic criterion, exhibit suitable volatile retention characteristics, and display a coherent backscatter opposition effect when sensed by radar, should be identified and targeted for future study.

Finally, we note that even if neutron or gamma ray spectrometers on the upcoming Lunar Prospector mission provide independent detection(s) of polar ice, high resolution topography within the south polar gap will be required to understand the geological context of permanent shadowing, *i.e.* to assess precise location and accessibility. Thus, efforts to obtain high resolution, geodetically-controlled topography of the lunar poles should be accorded high priority.

Acknowledgements. Eugene Shoemaker encouraged this work and offered helpful suggestions. James Arnold and Mark Robinson provided reviews that significantly improved the paper. This study was supported by the NASA Planetary Geology and Geophysics Program.

References

Arnold, J. R., Ice in the lunar polar regions, *J. Geophys. Res.*, *84*, 5659-5668, 1979.

Dickey, J. O., et al., Lunar laser ranging: A continuing legacy of the Apollo program, *Science*, *265*, 482-490, 1994.

Harmon, J. K. and M. A. Slade, Radar mapping of Mercury: Full-disk images and polar anomalies, *Science*, *258*, 640-643, 1992.

Ingersoll, A. P., T. Svitek and B. C. Murray, Stability of polar frosts in spherical bowl-shaped craters on the Moon, Mercury, and Mars, *Icarus*, *100*, 40-47, 1992.

Newhall, X. X., M. E. Standish and J. G. Williams, DE 102: A numerically integrated ephemeris of the Moon and planets spanning forty-four centuries, *Astron. Astrophys.*, *125*, 150-167, 1983.

Nozette, S., et al., The Clementine bistatic radar experiment, *Science*, *274*, 1495-1498, 1996.

Nozette, S., et al., The Clementine mission to the Moon: Scientific overview, *Science*, *266*, 1835-1839, 1994.

Paige, D. A., S. E. Wood and A. R. Vasavada, The thermal stability of water ice at the poles of Mercury, *Science*, *258*, 643-646, 1992.

Pike, R. J., Depth/diameter relations of fresh lunar craters: Revision from spacecraft data, *Geophys. Res. Lett.*, *1*, 291-294, 1974.

Salvail, J. R. and F. Fanale, Near-surface ice on Mercury and the Moon: A topographic thermal model, *Icarus*, *111*, 441-455, 1994.

Shoemaker, E. M., M. S. Robinson and E. M. Eliason, The south pole region of the Moon as seen by Clementine, *Science*, *266*, 1851-1854, 1994.

Smith, D. E., M. T. Zuber, G. A. Neumann and F. G. Lemoine, Topography of the Moon from the Clementine LIDAR, *J. Geophys. Res.*, *102*, 1591-1611, 1997.

Spudis, P. D., K. R. Stockstill, W. J. Ockels and M. Kruijff, Physical environment of the lunar south pole from Clementine data: Implications for future exploration of the Moon, *Lunar Planet. Sci. Conf.*, *XXVI*, 1339-1340, 1995.

Stacy, N. J. S. and D. B. Campbell, Stokes vector analysis of lunar radar backscatter, *IEEE Geosci. Remote Sens. Symposium (IGARSS '93)*, Tokyo, 30-32, 1993.

Stacy, N. J. S., D. B. Campbell and P. G. Ford, Arecibo radar mapping of the lunar poles: A search for ice deposits, *Science*, *276*, 1527-1530, 1997.

Turcotte, D. L., A fractal interpretation of topography and geoid spectra on the Earth, Moon, Venus and Mars, *J. Geophys. Res.*, *92*, E597-E601, 1987.

Ward, W. R., Past orientation of the lunar spin axis, *Science*, *189*, 377-379, 1975.

Watson, K., B. C. Murray and H. Brown, The behavior of volatiles on the lunar surface, *J. Geophys. Res.*, *66*, 3033-3045, 1961.

Williams, K. K. and M. T. Zuber, Measurement and analysis of major lunar basin depths from Clementine altimetry, *Icarus*, submitted, 1997.

Zuber, M. T., D. E. Smith, F. G. Lemoine and G. A. Neumann, The shape and internal structure of the Moon from the Clementine mission, *Science*, *266*, 1839-1843, 1994.

D.E. Smith, Laboratory for Terrestrial Physics, Code 920, NASA Goddard Space Flight Center, Greenbelt, MD 20771. (e-mail: dsmith@tharsis.gsfc.nasa.gov)

M.T. Zuber, Department of Earth, Atmospheric and Planetary Sciences, Massachusetts Institute of Technology, 54-518, Cambridge, MA 02139. (e-mail: zuber@tharsis.gsfc.nasa.gov)

(Received May 5, 1997; accepted June 13, 1997.)